

Stream-HLS: Towards Automatic Dataflow Acceleration

Suhail Basalama
basalama@ucla.edu

University of California, Los Angeles
Los Angeles, California, United States

Jason Cong
cong@cs.ucla.edu

University of California, Los Angeles
Los Angeles, California, United States

Abstract

High-level synthesis (HLS) has enabled the rapid development of custom hardware circuits for many software applications. However, developing high-performance hardware circuits using HLS is still a non-trivial task requiring expertise in hardware design. Further, the hardware design space, especially for multi-kernel applications, grows exponentially. Therefore, several HLS automation and abstraction frameworks have been proposed recently, but many issues remain unresolved. These issues include: 1) relying mainly on hardware directives (pragmas) to apply hardware optimizations without exploring loop scheduling opportunities. 2) targeting single-kernel applications only. 3) lacking automatic and/or global design space exploration. 4) missing critical hardware optimizations, such as graph-level pipelining for multi-kernel applications.

To address these challenges, we propose a novel methodology and framework on top of the popular multi-level intermediate representation (MLIR) infrastructure called Stream-HLS. Our framework takes a C/C++ or PyTorch software code and automatically generates an optimized dataflow architecture along with host code for field-programmable gate arrays (FPGAs). To achieve this, we developed an accurate analytical performance model for global scheduling and optimization of dataflow architectures. Stream-HLS is evaluated using various standard HLS benchmarks and real-world benchmarks from transformer models, convolution neural networks, and multilayer perceptrons. Stream-HLS designs outperform the designs of prior state-of-the-art automation frameworks and manually-optimized designs of abstraction frameworks by up to 79.43 \times and 10.62 \times geometric means respectively. Finally, the Stream-HLS framework is modularized, extensible, and open-sourced at <https://github.com/UCLA-VAST/Stream-HLS> (<https://doi.org/10.5281/zenodo.14585909>).

Keywords

FPGA; HLS; MLIR; Dataflow Architecture; MINLP; Streaming

1 Introduction

With the slowdown of Moore’s law [46] and the limits of Dennard’s scaling [5, 19], industry and academia have turned to specialized hardware architectures. Major tech companies developed their custom hardware accelerators as application-specific integrated circuits (ASICs) such as Google’s TPUs [28], or field-programmable gate arrays (FPGAs) such as Microsoft cloud projects [10, 15].

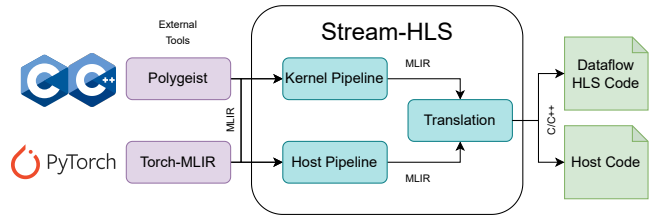


Figure 1: Stream-HLS Framework Overview

While designing hardware accelerators with hardware description languages (HDLs) such as Verilog and VHDL attain the best speedups and energy efficiency, this process demands significant hardware expertise and can span several months to years. Fortunately, advancements in high-level synthesis (HLS) have elevated the abstraction level from HDLs to C/C++. As a result, HLS combined with the reconfigurability of FPGAs [16] has enabled them to compete with GPUs and CPUs in various domains such as machine learning [3, 50, 60, 62], image processing [14, 25], genome sequencing [9, 36], and scientific computing applications [39, 54]. Despite this democratization of FPGA programming, designing high-performance accelerators with HLS still requires searching a huge design space and expertise in hardware design. To address these challenges, many prior works have focused on developing automation and abstraction tools and methodologies.

A typical HLS flow for accelerating a software application requires multiple iterations of code refactoring and transformation, as well as the insertion of directives (pragmas) to implement specific hardware optimizations, such as loop pipelining and loop unrolling. Furthermore, many software applications consist of multiple smaller tasks, known as kernels, such as matrix multiplication or the layers of a deep neural network (DNN). This makes optimizing multi-kernel applications more challenging, requiring global analysis, scheduling, and resource allocation for different kernels. Table 1 summarizes previous attempts towards abstracting and automating hardware design through HLS.

Numerous previous studies proposed automation tools that explore different aspects of the vast design space of transforming software applications into hardware accelerators. AutoDSE [48] and HARP [47], for instance, are state-of-the-art design space exploration tools that find the best hardware optimization directives

Framework (Venue)	Front-end	App. Domain	Multi-kernel Apps.	Loop Pipelining	Graph Pipelining (Streaming Dataflow)	Adaptive Parallelization	Performance Model
AutoDSE [48](TODAES'22)	C/C++	General	limited	✓	✗	✗	HLS Report
HARP [47](ICCAD'23)	C/C++	General	limited	✓	✗	✗	ML-based
SODA [12](ICCAD'18)	DSL	Stencils	✗	✓	✓	✓	Analytical
AutoSA [53](FPGA'21)	C/C++	Affine	✗	✓	✓	✓	Analytical
HeteroCL [30](FPGA'19)	Python/PyTorch	General	✓	Manual	✗	Manual	N/A
Allo [11](PLDI'24)	Python/PyTorch	Affine	✓	Manual	Manual	Manual	N/A
ScaleHLS [58](HPCA'22)	C/C++/PyTorch	Affine	✓	✓	✗	C/C++ only	Analytical
HIDA [59](ASPLOS'24)	C/C++/PyTorch	Affine	✓	✓	✗	C/C++ only	Analytical
POM [61](HPCA'24)	DSL	Affine	✓	✓	✗	✓	Analytical
Stream-HLS (this work)	C/C++/PyTorch	Affine	✓	✓	✓	✓	Analytical

Table 1: Stream-HLS Comparison with Prior Frameworks

(pragmas) to insert into the software application. These tools rely on another compiler called Merlin [56] to perform code refactoring suitable for HLS tools, but without changing the original code schedule. However, pragma/directive insertion without loop scheduling may not be sufficient to achieve good quality results. Furthermore, this line of work focuses on small applications with a single or a small number of kernels, such as those in the Polybench [44] suite.

Other works such as AutoSA [53] and SODA [12], introduced automated frameworks that convert C/C++ or domain-specific language (DSL) code into an optimized HLS code through both code transformation and pragma insertion. While these frameworks generate high-performance designs, their scope is limited to supporting only single-kernel applications (e.g., a single convolution layer). For multi-kernel applications, users need to manually integrate the different parts of the application. With the huge design space of global scheduling, this becomes a challenging task.

Other efforts, such as HeteroCL [30], and Allo [11], raise the level of abstraction for HLS from C/C++ to Python, allowing code transformation and directive optimizations within Python code. Although this approach enables the decoupling of algorithm design from the hardware optimization process at a higher level, it still necessitates the manual optimization of an expert to navigate the design space to produce high-performance designs.

Lastly, a few prior works built automated frameworks that can take multi-kernel applications and convert them into optimized dataflow designs by performing code transformation and pragma insertion, such as ScaleHLS [58], HIDA [59], and POM [61]. However, these frameworks lack two important aspects: 1) Streaming capabilities. 2) Global performance modeling for streaming architectures. Our work, Stream-HLS, falls under this category but produces globally optimized dataflow designs with streaming capabilities.

In this study, we present an end-to-end framework that takes a sequential multi-kernel program written in C/C++ or PyTorch and automatically converts it into an optimized HLS code representing a dataflow architecture as Figures 1 and 2b depict. While our methodology applies to FPGA and ASIC HLS tools, we use FPGAs for demonstration purposes.

The main contributions of our work are as follows:

- (1) an automatic, open-source, end-to-end framework to convert sequential multi-kernel applications into optimized parallel dataflow architectures with streaming capabilities;
- (2) an MLIR [33] library that performs multiple optimizations on a dataflow graph including dataflow canonicalization

and the conversion of shared buffers to FIFOs when possible;

- (3) an accurate performance model for dataflow architectures with shared-buffer and/or FIFO inter-task communications;
- (4) a global coordinated loop scheduling approach considering node-level pipelining, graph-level pipelining, and node-level parallelization using mixed integer nonlinear programming (MINLP);
- (5) a comprehensive evaluation against baseline models optimized by Vitis HLS [57] and other SOTA frameworks achieving geometric speedups between 5.42× and 2270.25×.

The paper starts with a motivating example (Section 2). Next, we present our methodology, detailing the process of converting sequential designs into parallelized dataflow architectures as well as our novel performance model and scheduling approach (Section 3). We then discuss the implementation of this methodology as an automated framework on top of MLIR (Section 4). Finally, we provide a comprehensive evaluation on a variety of benchmarks demonstrating the optimizations of Stream-HLS (Sections 5).

2 Motivation

Let us take a look at a simple multi-kernel application from the Polybench suite [44] called *3mm*. This application is composed of three matrix multiplications (gemm) where the outputs of the first two are used as input to the third matrix multiplication. Figure 2a shows the high-level dataflow graph for this benchmark. Given such a graph, the challenge we are tackling is how to automatically generate an optimized accelerator under hardware constraints.

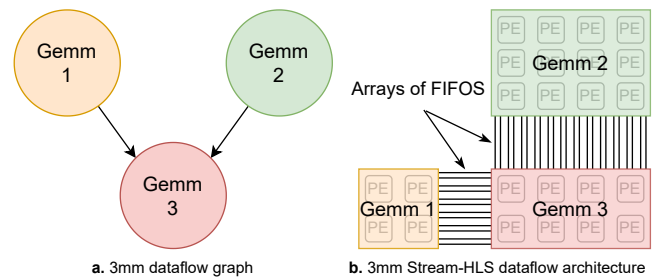


Figure 2: Dataflow Graph and Stream-HLS Architecture of *3mm* [44]

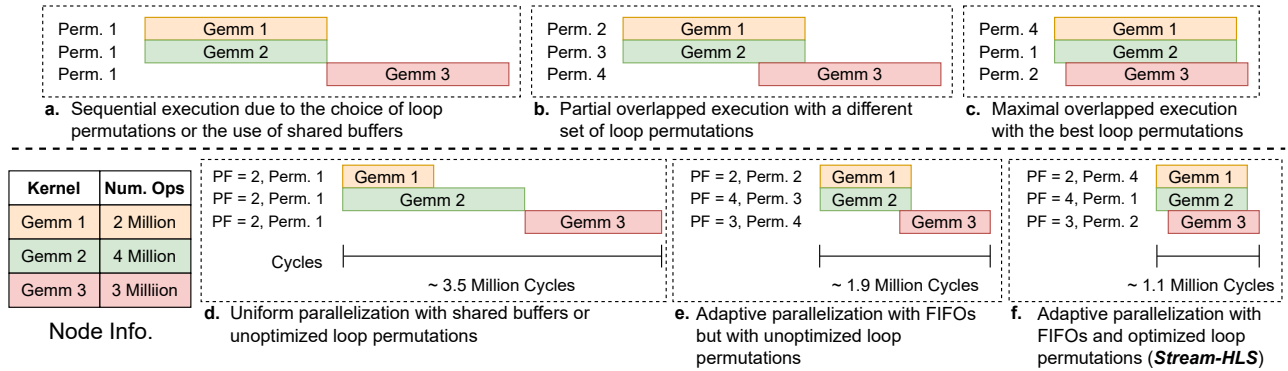


Figure 3: Execution $3mm$ Execution Traces under Different Loop Permutations and Parallelization Factors

We identified three critical but often conflicting optimizations that determine the overall performance. The design space for these optimizations, even for this simple example, is massive.

2.1 Node-level Pipelining

Loop pipelining is one of the most important optimizations in HLS. Ideally, with enough resources, a loop can be pipelined with an initiation interval (II) of 1; however, loop-carried dependencies (true data dependencies between write and read operations of consecutive iterations) may prohibit achieving an II of 1. One solution to this is to perform loop permutation that increases the dependence distance achieving an II of 1. For a *gemm* node (perfectly-nested loops of depth 3), there are $3! = 6$ permutations, four of which lead to an II of 1, and two (where the reduction loop is innermost) lead to an II greater than 1. Prior works such as ScaleHLS [58] and HIDA [59] address this issue by automatically permuting reduction loops to be the outermost for all nodes of an application dataflow graph, thus maximizing the loop-carried dependence distances. However, would this local optimization (i.e. for each node regardless of the whole dataflow graph) be always beneficial? This takes us to the next important optimization, namely, graph-level pipelining.

2.2 Graph-level Pipelining

Edges in a dataflow graph represent true data dependencies, and communication between nodes can occur via shared buffers or FIFO streaming channels. Using shared buffers requires dependent nodes to execute completely sequentially to avoid any dependency violations, which limit graph-level pipelining (Figure 3a). In contrast, streaming channels can be used to forward data elements that are ready before a node finishes its execution, enabling overlapped execution of dependent nodes as depicted in Figures 3b and 3c.

The feasibility of using streaming channels depends on the data order forwarded between nodes, which in turn is determined by the loop permutation of each node. Therefore, assessing the potential for overlapped execution requires examining the loop permutations across the entire graph. Figure 3a illustrates the execution traces for $3mm$, where nodes run sequentially, either due to mismatched data order or exclusive use of shared buffers, a common approach in prior work [30, 47, 48, 58, 59, 61]. Figure 3b presents a scenario where certain loop permutations enable partial overlap between *Gemm 1*, *Gemm 2*, and *Gemm 3* using streaming channels. Figure 3c shows an even more efficient set of permutations.

In this case, there are $3! \times 3! \times 3! = 216$ possible loop permutation combinations for this small graph, making it challenging for designers to find the optimal set that balances **node-level** and **graph-level pipelining**. Additionally, some commercial HLS tools, like Vitis HLS [57], may provide overly optimistic estimates for dataflow designs, which do not always reflect actual hardware performance. For example, Vitis HLS reports the same performance for designs in Figures 3b and 3c, but RTL simulations reveal the differences in their execution times.

2.3 Node-level Parallelization

The third optimization is parallelization within individual nodes of a dataflow graph. For high-performance accelerators, maximizing the use of computation resources, particularly DSPs (digital signal processing components), is essential. This can be achieved through complete loop unrolling, or partial loop unrolling using the divisors of loops' trip counts as done in [47, 48, 58, 59]. We call the product of the unroll factors of a node's loop nest the parallelization factor (*PF*). In single-kernel applications, parallelism is simply maximized by maximizing the kernel's *PF*. However, in multi-kernel applications, hardware resources must be distributed across the computation nodes in the dataflow graph. Using a single *PF* for all nodes in a graph can lead to imbalanced execution and under-utilization of hardware resources especially for imbalanced workloads, a scenario we call **uniform parallelization**. For example, in the $3mm$ example shown in Figure 3, a uniform *PF* of 2 results in a performance of around 3.5 million cycles (Figure 3d).

An alternative approach is **adaptive parallelization**, which assigns *PF*s proportional to each node's workload (Figures 3e and 3f). However, we found that adaptive parallelization alone is not always optimal because loop permutations still affect graph-level pipelining. For instance, even with the same adaptive parallelization, the design in Figure 3f outperforms the one in Figure 3e due to changing loop permutations.

Abstraction frameworks like HeteroCL [30], and Allo [11] require users to manually specify unroll factors for each node, which is challenging especially for multi-kernel applications. In the $3mm$ example, there are 5 parameters representing the problem size. For the $3mm$ medium case in the Polybench suite [44], these parameters are {180, 190, 200, 210, 220}, with {18, 8, 12, 16, 12} divisors, yielding a Cartesian product of 331,776 unique designs.

2.4 Design Space Size

The total design space, for this simple example, under these three optimizations, becomes $216 \times 331,776 = 71,663,616$ possible designs! Given only these three optimizations, two challenges arise:

- *How to estimate the performance of a dataflow design point with a mixture of shared-buffer and FIFO communication interfaces?*
- *How to search this huge design space?*

Stream-HLS addresses these two challenges by developing an accurate performance model capturing the three optimizations (including shared buffer and streaming interfaces) and formulates the design space exploration problem as solving MINLPs.

3 Methodology

3.1 Definitions and Preliminaries

Affine kernel is any computation algorithm consisting of arithmetic statements enclosed by nested loops where loop bounds and memory accesses are affine functions of the loop iterators [6].

Perfectly nested loops are loops that are entirely contained within one another without any intervening code, where only the innermost loop contains some statements.

Legal conversion of shared buffers to FIFOs requires two necessary conditions:

- Cond. 1.** The number of writes to a shared buffer must equal the number of reads from the buffer.
- Cond. 2.** The order a producer task writes data to the buffer must match the order in which a consumer task reads the data.

3.2 Input Program

Stream-HLS takes as input any arbitrary affine program consisting of a list of perfectly nested loops with constant loop bounds operating on multi-dimensional arrays (scalars and 1D arrays included). Arrays can have arbitrary affine references (reads or writes) in any loop nest. Many of the common targets for hardware acceleration are applications that can be represented as affine programs. This encompasses a wide variety of layers and kernels used in real-world DNNs and scientific computing applications such as data reshaping/transformation, matrix multiplication, dot product, convolution, pooling, activation layers (ReLU, GeLU, Sigmoid), softmax, batch normalization, piecewise add and multiply, to mention a few.

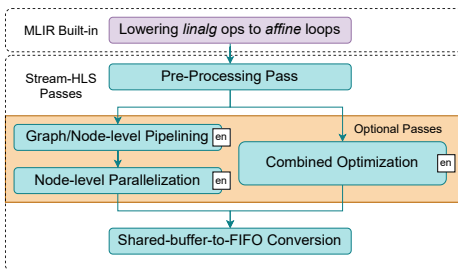


Figure 4: Main Passes of Stream-HLS Kernel Pipeline

3.3 Pre-Processing Pass

3.3.1 Dataflow Canonicalization. The first step in our methodology is to make a program dataflow compatible. Some HLS tools

impose rules a program must meet before it can be implemented as a canonical dataflow architecture. One rule is that all shared buffers must have a single-producer-single-consumer relationship. Thus, this step converts all single-producer-multi-consumer or multi-producer-multi-consumer shared buffers into single-producer-single-consumer shared buffers by duplicating the shared buffers. Figure 5 illustrates this process.

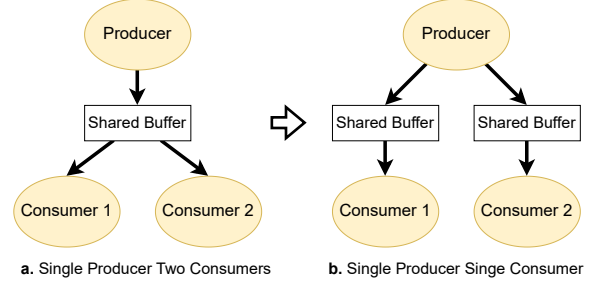


Figure 5: Dataflow Canonicalization

3.3.2 Addressing Cond. 1. Many of the nodes of an application involve some data reuse in their input or output arrays. Let us take a simple example of matrix multiplication followed by matrix addition as shown in Listing 1.

```

1 float C[32][32];
2 L1: for(int i = 0; i < 32; i++)
3   L2: for(int j = 0; j < 32; j++)
4     L3: for(int k = 0; k < 32; k++){
5       float a = A[i][k];
6       float b = B[k][j];
7       float c = C[i][j];
8       float tmp = c + a * b;
9       C[i][j] = tmp;
10    }
11 L4: for(int j = 0; j < 32; j++)
12   L5: for(int i = 0; i < 32; i++)
13     E[i][j] = C[i][j] + D[i][j];
  
```

Listing 1: Original Code for Matrix Multiplication Followed by Matrix Addition

Notice that array C is written to 32^3 times in the first loop nest and is read only 32^2 times in the second loop nest. In the first loop nest, the C array is reused locally 32 times by the innermost loop (commonly known as a reduction loop) with induction variable k . To satisfy **Cond. 1**, we transform the code such that only the final values (when $k = 31$) of the array C are written to a new buffer. Thus, in conjunction with the canonicalization step, we transform the code into the one shown in Listing 2.

In this new equivalent code, array $C_shared_buff_2$ is written exactly 32^2 times and read 32^2 times, satisfying **Cond. 1**.

Dataflow canonicalization and addressing **Cond. 1** are performed jointly in the pre-processing pass in Figure 4.

3.4 Shared-buffer-to-FIFO Conversion

3.4.1 Addressing Cond. 2. We utilize the concept of an access function (AF), which is a mapping from the loop induction variables to the indices of the array reference. For example, the write access function (WAF) of the store operation in line 15 of Listing 2 is $(i, j, k) \rightarrow (i, j)$, and since the k induction variable is not used, the

```

1 float C_shared_buff_1[32][32];
2 float C_shared_buff_2[32][32];
3 float C_local_buff[32][32];
4 L1: for(int i = 0; i < 32; i++){
5     L2: for(int j = 0; j < 32; j++){
6         L3: for(int k = 0; k < 32; k++){
7             float a = A[i][k];
8             float b = B[k][j];
9             if(k==0)
10                C_local_buff[i][j] = C_shared_buff_1[i][j];
11            float c = C_local_buff[i][j];
12            float tmp = c + a * b;
13            C_local_buff[i][j] = tmp;
14            if(k==31)
15                C_shared_buff_2[i][j] = C_local_buff[i][j];
16        }
17    L4: for(int j = 0; j < 32; j++){
18        L5: for(int i = 0; i < 32; i++){
19            E[i][j] = C_shared_buff_2[i][j] + D[i][j];

```

Listing 2: Transformed Version of Code in Listing 1

access function simplifies to $(i, j) \rightarrow (i, j)$. Similarly, the read access function (RAF) of the load operation (line 19) is $(j, i) \rightarrow (i, j)$.

Now, we compare the write and read access functions. If they are equivalent, then the shared buffer can be safely replaced by a FIFO. In this example, since the functions are not equivalent, the shared buffer is retained. Nevertheless, we can see that permuting (interchanging) the $L1$ and $L2$ loops or the $L4$ and $L5$ loops makes the two access functions equivalent ($WAF = RAF$) and the shared buffer can be safely replaced with a FIFO. This brings us to the optional code transformation and performance modeling passes shown in the orange area in Figure 4.

3.5 Performance Modeling

To perform any meaningful optimization, a performance model of dataflow architectures is needed.

3.5.1 Dataflow Graph. In this step, a directed acyclic graph (DAG) is constructed to represent an application where:

- **Node** represents a perfect loop nest with some statements representing a high-level operation such as matrix multiplication or DNN layers.
- **Edge** is a read-after-write (true/flow) dependency between nodes as Figure 6 depicts.

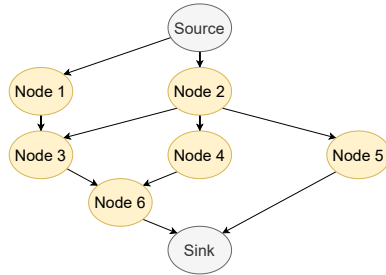


Figure 6: Dataflow Graph Example

Nodes can have an arbitrary number of different inputs and a single output. The single output can then be an input to one or more other nodes. Each node n contains critical information relevant to its performance in hardware (see Table 2).

Symbol	Description
II_n	Achievable initiation interval
U_n	Number of DSPs used for arithmetic operations
$LR_n^{n'}$	Relative* time of last read from input node n'
$RAF_n^{n'}$	Read access function from input node n'
FW_n	Relative* time of first write to the output
LW_n	Relative* time of last write to the output
WAF_n	Write access function to the output

* relative to the absolute starting time $st(n)$ of the node

Table 2: Node Information

The achievable initiation interval (II_n) and DSP factor (U_n) are calculated based on characteristics of the loop nest and memory references, and the type of arithmetic operations it contains. The times of the last read ($LR_n^{n'}$), first write (FW_n), and last write (LW_n) are extracted from the order (permutation) of the loop nest and the achievable II . We define a time function $t(\text{indices})$ that takes the indices (locations) of a cell of an array and returns a scalar number representing the time of that access. The function is calculated utilizing the order of the loops and their upper and lower bounds. For example, let us consider the first loop nest in Listing 2 to be node n . The time of the first and last writes to $C_shared_buff_2$ (line 15) are calculated using a time function as follows: $t(i, j, k = 31) = II_n(32^2i + 32j + k) \Rightarrow t(i, j) = II_n(32^2i + 32j + 31)$. Then, $FW_n = t(0, 0) = 31 \times II_n$ and $LW_n = t(31, 31) = 32767 \times II_n$. Note that these time equations depend on two things:

- The permutations of the loops containing the memory access.
- The bounds of the loops containing the memory access.

This will be relevant for the performance model and the three optimizations we discussed in the motivation section.

3.5.2 Performance Model Equations. Next, we sort the DAG in a topological order, and for each node n , we calculate three equations as shown in Table 3.

Equation
$st(n) = \max_{n' \in \text{ins}(n)} (\text{Arrives}(n, n'))$
where:
$\text{Arrives}(n, n') = \begin{cases} fw(n') & \text{if } WAF_{n'} = RAF_n^{n'} \\ lw(n') & \text{otherwise} \end{cases}$
$fw(n) = st(n) + FW_n$
$lw(n) = \max_{n' \in \text{ins}(n)} (\text{Depend}(n, n') + \text{Epilogue}(n, n'))$
where:
$\text{Depend}(n, n') = \max(st(n) + LR_n^{n'}, lw(n'))$
$\text{Epilogue}(n, n') = LW_n - LR_n^{n'}$
$\text{ins}(n)$ is the set of input nodes of node n .

Table 3: Performance Model Equations

- $st(n)$ represents the absolute starting time of node n . A node cannot start execution until it has data on all its incoming edges. If a buffer can be replaced with a FIFO ($WAF_{n'} = RAF_n^{n'}$), then its arrival time is the absolute time of the first write by its predecessor node n' , otherwise (i.e., when a shared buffer cannot be replaced with a FIFO), the arrival time is the absolute end time of its predecessor node n' , which is equal to the last write $lw(n')$.

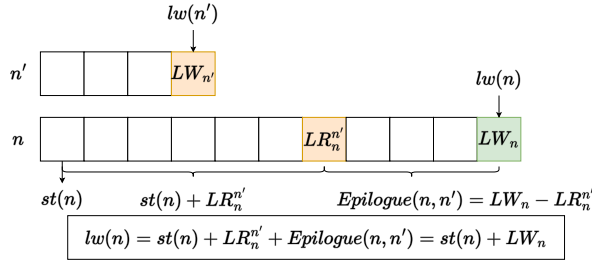


Figure 7: The First Case of the $lw(n)$: when a predecessor node n' produces its data before node n consumes it

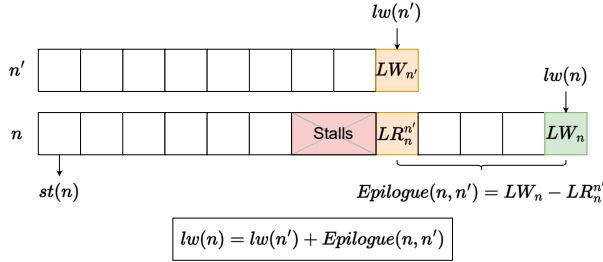


Figure 8: The Second Case of the $lw(n)$: when a consumer node n must wait (stall) for data from its predecessor node n'

- $fw(n)$ represents the absolute time for the first write of node n . It is calculated as the sum of the absolute starting time of the node ($st(n)$) and the relative first write time FW_n .

- $lw(n)$ represents the absolute time for the last write performed by node n , marking the time the node finishes its execution. For each incoming node n' , we need to calculate two terms:

- $Epilogue(n, n')$ represents the remaining time after the last read by the current node n .

- $Depend(n, n')$ represents the time of the last read performed by node n , which is either the sum of the absolute starting time of n and the relative time of its last write (when the write happens before the read as Figure 7 depicts), or it is the absolute time of the last write performed by its predecessor node n' plus the epilogue defined above since the last read of the current node cannot happen before the last write of the predecessor node as depicted in Figure 8.

The last write done by node n (i.e., the end time of its execution) is then calculated as the maximum of the two terms above for all the incoming nodes. The total execution time of a dataflow graph is the time of the last write by the last node in the graph. For instance, the total execution time of the dataflow graph in Figure 6 is $lw(Sink)$. With a closed-form formula to estimate the performance of a design point (dataflow architecture), we can now optimize the code using the performance model as an objective function.

3.6 Graph/Node-level Pipelining

The achievable II_n of each node and the degree of inter-node (graph-level) concurrency/pipelining is determined by the loop ordering of the loop nests of each node in the program. Therefore, for each node n with d nested loops in the dataflow graph, $d!$ binary indicator variables (B_n) are created to represent all loop permutations for

Expanded Equation	
$st(n) = \max_{n' \in ins(n)} \left(\sum_{b \in B_n} \sum_{b' \in B_{n'}} Arrives(n, n') \times b \times b' \right)$	
where:	
$Arrives(n, n') = \begin{cases} fw(n') & \text{if } WAF_{n'} = RAF_n^{n'} \\ lw(n') & \text{otherwise} \end{cases}$	
$fw(n) = st(n) + \sum_{b \in B_n} FW_n \times b$	
$lw(n) = \max_{n' \in ins(n)} (Depend(n, n') + Epilogue(n, n'))$	
where:	
$Depend(n, n') = \max(st(n) + \sum_{b \in B_{n'}} LR_n^{n'} \times b, lw(n'))$	
$Epilogue(n, n') = \sum_{b \in B_n} (LW_n - LR_n^{n'}) \times b$	

$ins(n)$ is the set of incoming nodes of node n .

B_n is the set of binary indicator variables of node n .

Table 4: Expanded Performance Model Equations

that node. Note that different permutations of a node result in different values for the node information in Table 2. Thus, for each equation in the performance model, we augment the constants by multiplying them with the indicator variables as detailed in Table 4.

For the starting time $st(n)$, we must consider the relationship between the producer and consumer nodes to determine whether a FIFO can be used or not (see the term $Arrives(n, n') \times b \times b'$) in Table 4. Finally, the MINLP program is constrained by making the sum of the indicator variables of each node equal 1 to choose one specific loop permutation. After solving the program, we perform a loop permutation on each node using the found solution. Equation 1 shows the objective function and constraints of the first MINLP.

$$\begin{aligned} \min_{b \in B_n} \quad & lw(Sink) \quad \forall n \in G \\ \text{s.t.} \quad & \sum_{b \in B_n} b = 1 \quad (\text{Perm. Const.}) \end{aligned} \quad (1)$$

```

1 L1_1: for(int i1 = 0; i1 < 32/Ti; i1++)
2 L2_1: for(int j1 = 0; j1 < 32/Tj; j1++)
3 L3_1: for(int k1 = 0; k1 < 32/Tk; k1++)
4 #pragma HLS Pipeline
5 L1_2: for(int i2 = 0; i2 < Ti; i2++) //unroll
6 L2_2: for(int j2 = 0; j2 < Tj; j2++) //unroll
7 L3_2: for(int k2 = 0; k2 < Tk; k2++) //unroll
8 //...omitted for brevity, i=i1*Ti+i2, j=j1*Tj+j2
9 if(k1 == (32/Tk) - 1)
10 fifos_2d[i2][j2].write(C_local_buff[i][j]);
11 L5_1: for(int i1 = 0; i1 < 32/Ti; i1++)
12 L4_1: for(int j1 = 0; j1 < 32/Tj; j1++)
13 #pragma HLS Pipeline
14 L5_2: for(int i2 = 0; i2 < Ti; i2++) //unroll
15 L4_2: for(int j2 = 0; j2 < Tj; j2++) //unroll
16 // i=i1*Ti+i2, j=j1*Tj+j2
17 E[i][j] = fifos_2d[i2][j2].read() + D[i][j];

```

Listing 3: Tiled and Parallelized Version of Code in Listing 2 with Array of FIFOs Communication

3.7 Node-level Parallelization

So far, our analysis has been based on the granularity of single elements of data (scalars), so at a first glance, it seems our performance model does not consider the parallelization within each node. Nevertheless, if we think about the problem at the granularity of

tiles of data, we can apply the same analyses on multi-dimensional tiles of data, rather than on scalars. To illustrate, let us look at the code in Listing 3. It is a tiled version of the code shown in Listing 2 (each loop is split into Lx_1 , and Lx_2). Node-level parallelization is then achieved through unrolling the innermost loops and sending tiles of data between nodes, rather than single scalar values. Tiles of data are then communicated through partitioned shared buffers or using arrays of FIFOs (see Figure 2b and lines 10 and 17 in Listing 3). Another important aspect to consider is the tile size between dependent nodes. In order to keep an execution similar to the unparallelized code, we need to use the same tiling factors (Ti and Tj) between dependent nodes depicted in Listing 3. Now, we can reason about a tiled program in a similar way to the original unparallelized one, but with variable loop bounds ($32/Ti, 32/Tj, 32/Tk$). Therefore, the node information in Table 2 become symbolic formulas in terms of the variable tiling factors. The values of these tiling factors (Ti, Tj, Tk) are to be found by another augmented performance model which is omitted for space. The new MINLP is shown in Equation 2.

$$\begin{aligned}
 & \min_{x \in X_n} lw(\text{Sink}) && \forall n \in G \\
 & \text{s.t. } x = x' && (\text{Tile Size Const.}) \\
 & ub \% x = 0 && (\text{Divisor Const.}) \\
 & \sum_{n \in G} (U_n \prod_{x \in X_n} x) \leq DSPs && (\text{DSP Const.})
 \end{aligned} \tag{2}$$

Where: $x' \in X_{n'}, n' \in \text{ins}(n)$
 x and x' refer to the same array dimension.
 ub is the upper bound of the target loop.

For each node n with d nested loops in the dataflow graph, we create d integer variables (X_n) to represent the tiling factors. The first constraint enforces the tile sizes between dependent nodes are equal, the second constraint enforces the tiling factors to be divisors of the loop bounds, and the last constraint ensures that the DSP utilization does not exceed the available DSPs of a given FPGA. U_n is a factor that depends on the type of arithmetic operations and their hardware utilization.

3.8 Combined Optimization

The previous two MINLPs can be used to find loop permutations and then tiling factors separately. The first MINLP explores the design space of node/graph-level pipelining, and the second MINLP explores the design space of node-level parallelization. However, since these two optimizations are interconnected, solving each MINLP separately may lead to sub-optimal solutions. Therefore, we create a third MINLP to explore the whole design space to capture both optimizations at once as shown in Equation 3, which aims to find d binary variables (B_n) and d integer variables (X_n) representing loop permutation and tiling factors of a node n .

4 Implementation

4.1 MLIR Background

MLIR (multi-level intermediate representation) [33, 34] is a sub-project of the famous LLVM compiler infrastructure [32] that has

$$\begin{aligned}
 & \min_{b \in B_n, x \in X_n} lw(\text{Sink}) && \forall n \in G \\
 & \text{s.t. } \sum_{b \in B_n} b = 1 && (\text{Perm. Const.}) \\
 & x = x' && (\text{Tile Size Const.}) \\
 & ub \% x = 0 && (\text{Divisor Const.}) \\
 & \sum_{n \in G} (U_n \prod_{x \in X_n} x) \leq DSPs && (\text{DSP Const.})
 \end{aligned} \tag{3}$$

Where: same as Equation 2

been gaining popularity in the industry and academia. The novel idea of MLIR is the concept of *dialects*, which is a collection of operations, types, and attributes to represent semantics at a specific level of abstraction, thus the name multi-level intermediate representation. MLIR includes many built-in dialects, such as the *linalg* dialect that represents linear algebra operations like matrix multiplication and convolution. Another useful built-in dialect is the *affine* dialect suitable for affine kernels, which enables efficient and reliable dependence analysis and loop transformations.

4.2 External Tools

To find solutions to our scheduling mathematical programs, we use the AMPL [42] interface with the Gurobi solver [43]. Further, Stream-HLS utilizes two external tools as front-ends for translating code into MLIR: 1) **Torch-MLIR** [35] for translating a PyTorch model into *linalg* MLIR, and 2) **Polygeist** [38] for translating C/C++ into *affine* MLIR (see Figure 1).

4.3 Stream-HLS Implementation

Stream-HLS mainly utilizes four built-in dialects: *linalg*, *affine*, *mem-ref*, *arith*. Stream-HLS also adopts an updated version of an HLS dialect developed by prior works [58, 59] for HLS-specific operations. In addition, for node-level parallelization, we created new types and operations to represent multi-dimensional array of streams/-FIFOs that can be referenced using affine maps. The Stream-HLS library is written in C++ with more than 40K lines of code and is modularized enabling further development and extensions in the future. Stream-HLS has three main components described below.

4.3.1 Host Pipeline. While the MLIR infrastructure always ensures the validity of the IR at any point of the compiler passes, it is the responsibility of the developer to maintain the semantic equivalence of the program. A verification pipeline composed of compiler passes has been developed for this purpose. The pipeline takes the input program’s IR (and model parameters for DNNs) and creates host code with a testbench comparing the outputs of the original software code with the outputs of the generated design.

4.3.2 Kernel Pipeline. The kernel pipeline consists of the critical conversion and scheduling passes implementing the ideas discussed in the previous section.

4.3.3 Translation. After transforming the original program into a host MLIR and kernel MLIR, the MLIRs are translated into C++ Vitis HLS code. The translation modules are based on the one developed by [58, 59]. In addition to Vitis HLS, we developed translation for a SOTA HLS library called TAPA [13] built for dataflow designs.

Application	Opt1 (Shared-buffers to FIFOs only)			Opt5 (Combined Optimization)		
	RTL Cycles	Stream-HLS Cycles	Vitis Cycles	RTL Cycles	Stream-HLS Cycles	Vitis Cycles
Autoencoder	2.98E+07	2.68E+07 (0.90×)	2.57E+07 (0.86×)	3.92E+04	3.62E+04 (0.92×)	3.31E+04 (0.84×)
Residual MLP	1.84E+07	1.84E+07 (1.00×)	1.68E+07 (0.91×)	3.98E+04	3.31E+04 (0.83×)	3.30E+04 (0.83×)
Residual Block	5.79E+07	5.79E+07 (1.00×)	2.91E+07 (0.50×)	2.09E+06	1.05E+06 (0.50×)	1.83E+06 (0.88×)
DWSConv. Block	6.63E+06	6.53E+06 (0.98×)	3.82E+06 (0.58×)	1.35E+05	8.42E+04 (0.63×)	1.34E+05 (1.00×)
Feed Forward	6.73E+07	6.73E+07 (1.00×)	6.71E+07 (1.00×)	6.60E+04	6.58E+04 (1.00×)	6.56E+04 (0.99×)
Multi-Head Self Attention	1.05E+07	1.06E+07 (1.00×)	1.05E+07 (1.00×)	3.51E+04	3.51E+04 (1.00×)	3.47E+04 (0.99×)
3mm	6.38E+07	6.38E+07 (1.00×)	6.38E+07 (1.00×)	4.91E+04	4.90E+04 (1.00×)	4.80E+04 (0.98×)
atax	1.28E+06	1.28E+06 (1.00×)	8.00E+05 (0.63×)	2.18E+03	2.10E+03 (0.97×)	1.14E+03 (0.52×)
7mm Balanced	1.15E+06	1.15E+06 (1.00×)	1.05E+06 (0.92×)	5.68E+03	5.54E+03 (0.97×)	4.24E+03 (0.75×)
7mm Imbalanced	4.29E+06	4.24E+06 (0.99×)	4.19E+06 (0.98×)	1.00E+04	9.20E+03 (0.92×)	8.35E+03 (0.83×)
Geo. Mean		0.99×	0.81×		0.85×	0.85×

Table 5: Stream-HLS Performance Model Prediction vs. Vitis HLS Prediction Compared to RTL Simulation Cycle Count

4.3.4 *End-to-End Compilation.* Stream-HLS is fully automated and open-source. The framework takes a PyTorch model or C/C++ code as input, and with a push of a button, produces an optimized dataflow architecture C/C++ code along with host code that verifies the correctness of the implementation against the software golden results. Figure 1 illustrates a high-level overview of our framework.

5 Evaluation

In this section, we validate the Stream-HLS performance model, evaluate Stream-HLS against Vitis HLS [57] baseline and prior works, and provide an in-depth evaluation of the different optimizations of Stream-HLS. All experiments are performed using Vitis HLS 2023.2 [57] targeting AMD Alveo U280 Data Center Accelerator Card [55] at 300MHz.

5.1 Experimental Setup and Benchmarks

We conducted experiments on five categories of applications: 1) seven kernels from the Polybench benchmark suite [44]. 2) multi-head self attention and feed forward network found in transformer models [51]. 3) A residual block [21] and a depthwise separable convolution block (DWSConv.) [23](involving standard convolution, depthwise convolution, pointwise convolution, batch normalization, and ReLU activation). 4) Two multilayer perceptron (MLP) networks: an encoder-decoder MLP [52], and a 4-layer MLP with a residual connection. 5) Two synthetic 7 matrix multiplication kernels connected in series (7mm). For each application we conducted 5 experiments using different optimization levels of Stream-HLS as shown in Table 6. For all MINLPs, we set a timeout of 20 minutes and 2560 DSPs limit¹ for the MINLP solver. All solutions were found in less than 2 minutes, except for **Opt4** and **Opt5** of the residual block and multi-head self attention block where they reached the 20 minute timeout due to the size of the design space. Due to the inaccuracies of Vitis HLS reports for dataflow designs, we conducted all experiments using RTL cycle-accurate simulation.

Optimization	Opt1	Opt2	Opt3	Opt4	Opt5
Shared-buffers to FIFOs	✓	✓	✓	✓	✓
Graph/Node-level Pipelining	✗	✓	✗	✓	✓
Node-level Parallelization	✗	✗	✓	✓	✓
Combined Optimization	✗	✗	✗	✗	✓

Table 6: Different Levels of Optimizations of Stream-HLS

¹Slightly less than the DSPs of a single super logic region (SLR) of the U280 FPGA

5.2 Performance Model Validation

To validate the performance model, we chose designs under **Opt1** and **Opt5**. **Opt1** designs are the baseline designs featuring a random level of graph/node-level pipelining determined by the original order of the loop nests with a mixture of shared buffers and FIFO interfaces. This can help us show the accuracy of our performance model under random configuration. Additionally, we show the predictions of our performance model for the fully-optimized designs (**Opt5**). For the randomized **Opt1** designs, Stream-HLS predictions are very close to the actual RTL simulation cycles while Vitis HLS estimates can be 0.50× of the actual RTL simulation cycles. We suspect that such optimistic estimates of Vitis HLS are due to the use of a simplified performance model for dataflow designs that uses the slowest node as the latency of the whole design. For **Opt5** designs, Stream-HLS predictions may not match the actual RTL simulation. The reason for this is that with node-level parallelization, Vitis HLS may not achieve the requested II for some nodes leading to a higher II than our performance model prediction. This is a difficult problem since the Vitis HLS compiler performs further code instrumentation that are hard to predict. In fact, with some manual code refactoring related to the coding style (without changing the schedule), Vitis HLS can achieve the expected II, but this is not automated yet in our framework and will be improved in the next version of Stream-HLS. Furthermore, we have noticed that the degradation in II is relative. For instance, if Stream-HLS predicts the II of a specific loop nest to be 1 for permutation 1 and 4 for permutation 2, then the achieved II by Vitis HLS for permutation 1 is lower (better) than the achieved II for permutation 4.

5.3 Comparison with Prior Works

In this subsection, we compare Stream-HLS with manually and automatically optimized designs generated by similar state-of-the-art frameworks. Allo [11] and HeteroCL [30] are abstraction frameworks that enable a user to optimize a schedule manually through schedule optimization primitives, such as loop reordering (permutation), loop pipelining, and loop unrolling. What is unique about Allo compared to HeteroCL is the *compose* primitive, which enables graph-level pipelining through streaming channels for multi-kernel applications. HIDA [59], ScaleHLS [58] and POM [61] are automatic hardware compilers that take a C/C++ or PyTorch model (or DSL for POM) and automatically generate HLS designs. However, these frameworks have two limitations: 1) They adopt shared buffers only

App. [44] Medium	Stream-HLS (Opt5)			Manually Optimized (Speedup [*])		Automatically Optimized (Speedup [*])			
	(220, 2560, 9024) DSPs			Allo [11]	HeteroCL [30]	HIDA [59]	ScaleHLS [58]	POM [61]	Vitis HLS [57]
2mm	3.78E+5	3.64E+4	1.18E+4	2.68E+5 (7.38×)	4.81E+5 (13.22×)	2.46E+5 (6.75×)	2.46E+5 (6.75×)	1.98E+6 (54.38×)	1.18E+8 (3236.36×)
3mm	6.02E+5	4.91E+4	1.44E+4	2.23E+5 (4.54×)	4.65E+5 (9.47×)	2.79E+5 (5.69×)	2.66E+5 (5.42×)	2.03E+6 (41.45×)	1.28E+8 (2600.83×)
atax	1.59E+4	2.18E+3	2.18E+3	8.82E+3 (4.05×)	2.92E+4 (13.39×)	1.34E+4 (6.15×)	1.93E+4 (8.85×)	Failed	1.29E+6 (591.09×)
bicg	8.03E+3	1.11E+3	1.11E+3	1.65E+3 (1.48×)	2.88E+3 (2.59×)	1.44E+4 (12.99×)	1.44E+4 (12.99×)	Failed	1.28E+6 (1150.72×)
gemm	3.30E+5	2.41E+4	7.10E+3	2.39E+5 (9.92×)	2.36E+5 (9.81×)	1.77E+5 (7.36×)	1.77E+5 (7.36×)	1.33E+6 (55.34×)	1.06E+7 (441.14×)
gesummv	3.18E+3	6.73E+2	6.73E+2	1.54E+3 (2.29×)	1.79E+3 (2.66×)	6.32E+3 (9.38×)	6.32E+3 (9.40×)	6.58E+3 (9.78×)	5.00E+5 (742.97×)
mvt	8.04E+3	6.67E+2	5.50E+2	4.68E+2 (0.70×)	2.08E+3 (3.12×)	1.01E+4 (15.08×)	1.51E+4 (22.60×)	4.00E+4 (60.02×)	2.56E+6 (3838.11×)
Geo. Mean for 220 DSPs Limit (POM)				0.35×	0.68×	0.93×	1.03×	3.74×	145.45×
Geo. Mean for 2560 DSPs Limit (1 SLR)				3.17×	6.20×	8.50×	9.42×	37.40×	1325.85×
Geo. Mean for 9024 DSPs U280 Limit				5.42×	10.62×	14.55×	16.13×	79.43×	2270.25×

* Speedups compared to Stream-HLS Opt5 with the 2560 DSPs limit for one super logic region (SLR)

Table 7: RTL Simulation Cycle Count Comparison with Prior Abstraction and Automation Frameworks

for inter-task communication, which limits graph-level pipelining. 2) Automatic design space exploration is only available for the C/C++ and DSL front-ends, while the PyTorch front-end lacks DSE capabilities and requires a user to specify a single unroll factor to be applied for all loop nests (uniform parallelization).

For Allo and HeteroCL, we used designs manually optimized by the tools’ authors targeting the same U280 FPGA. For HIDA, ScaleHLS, and POM we used their C/C++ and DSL front-ends to perform design space exploration to find the best designs targeting the U280 FPGA with the maximum 9024 DSP limit (whole board). For Vitis HLS [57] baseline designs, we did not perform any optimization except for the default pipelining applied by Vitis HLS. For Stream-HLS, we generated the designs using the combined optimization **Opt5** under three different DSP limit constraints 220, 2560 (single SLR), and 9024 DSPs. All designs finished RTL simulation except: 1) Allo’s **3mm** design, which ran into an infinite loop during the simulation, so we used cycles reported by Vitis HLS instead. 2) POM’s **atax** and **bicg** designs, which failed during the DSE step with internal errors. Further, we also noticed that POM does not exceed the 220 DSP limit used in their paper despite setting the 9024 DSP limit in the configuration file, thus we added the 220 DSP limit experiments for Stream-HLS for a fair comparison.

Table 7 shows the absolute RTL cycles and the speedups of Stream-HLS designs over the prior frameworks. We can see that Stream-HLS designs are better or comparable to designs manually optimized by an expert in the case of Allo and HeteroCL at different DSP limits. The reason for this is that design space even for small applications can grow exponentially, making it difficult for a human experts to find the set of optimizations to apply. Conversely, Stream-HLS designs constantly outperform the designs of HIDA, ScaleHLS starting at the 1 SLR DSP limit and the designs of POM even at the 220 DSP limit. We believe this is due to the lack of graph-level pipelining and/or their performance modeling with the iterative DSE algorithms employed by these frameworks.

Additionally, we compare the scalability of Stream-HLS MINLP DSE under the three DSP constraints with HIDA’s [59] (which uses the same DSE of ScaleHLS [58]) and POM’s [61] iterative DSEs. We also compare the DSP percentage utilization of the three frameworks as depicted in Table 8. The runtime of Stream-HLS DSE outperforms HIDA’s [59] DSE with a geometric mean of 176.41×. POM’s DSE runtime is similar to ours, but it produces inferior designs. In terms of DSP allocation, Stream-HLS constantly maximizes DSP utilization under the specified limit and problem size

App.	Stream-HLS (Opt5)		HIDA [59]		POM [61]	
	DSE(s)	DSPs(%)	DSE(s)	DSPs(%)	DSE (s)	DSPs(%)
2mm	(7, 4, 4)	(2.5, 21.5, 82.4)	644	10.7	4	0.7
3mm	(6, 6, 4)	(2.5, 27.8, 88.9)	1501	6.9	8	1.0
atax	(4, 3, 3)	(2.2, 16.6, 16.6)	45	1.7	-	-
bicg	(3, 7, 3)	(2.2, 16.6, 16.6)	708	1.3	-	-
gemm	(4, 4, 3)	(2.1, 28.3, 92.0)	1775	3.6	1	0.6
gesummv	(4, 3, 4)	(2.4, 10.2, 10.2)	839	2.0	2	1.1
mvt	(3, 4, 4)	(2.2, 25.6, 39.7)	825	1.8	2	0.5
DSE Runtime Geo. Mean Speedup			176.41×		0.74×	

DSE runtime speedups are measured over the 9024 DSPs limit
Table 8: DSE Runtimes in Seconds and DSP Utilization under (220, 2560, 9024) DSP Limits

constraints thanks to our global scheduling approach. Conversely, under the same DSE configuration, HIDA and POM yield variable DSP utilization for different applications.

Node (Ops)	Opt5 - 2560		HIDA		Opt5 - 220		POM	
	Lat.	DSPs	Lat.	DSPs	Lat.	DSPs	Lat.	DSPs
Gemm1(1.37E+7)	4.56E+4	752	1.14E+5	303	5.70E+5	63	8.55E+5	43
Gemm2(1.76E+7)	4.39E+4	1001	1.46E+5	33	4.39E+5	101	1.10E+6	3
Gemm3(1.44E+7)	4.79E+4	753	1.33E+5	17	5.99E+5	62	8.98E+5	3
Total (4.56E+7)	4.91E+4	2507	2.79E+5	623	6.02E+5	227	2.03E+6	92

Table 9: 3mm Latency and DSP Count Breakdown

Lastly, Table 9 breaks down the latencies and DSP utilization of the three nodes of **3mm**. We can see that under a specific DSP limit, Stream-HLS distributes the DSP resources among the three nodes while maximizing graph/node-level pipelining resulting in a total latency close to that of the slowest node. The DSEs of HIDA and POM result in a less even distribution of DSPs² and a sequential execution between **Gemm 1** or **Gemm 2** and **Gemm 3** due to the lack of graph-level pipelining confirming our motivation example in Figure 3.

5.4 Different Optimizations of Stream-HLS

To isolate the impact of different Stream-HLS optimizations, we generate five designs for each application starting with only replacing shared buffers with FIFOs as a baseline (refer to Table 6). We can see that optimizing loop order only (**Opt2**) can help maximize graph/node-level pipelining, achieving between 3.91× and 7.28× speedups. Next, applying node-level parallelization without considering loop order (**Opt3**) leads to speedups between 7.99× and 63.85×. **Opt4** first optimizes loop order to maximize graph/node-level pipelining and then optimizes node-level parallelization in two

²Total DSPs include top-level DSPs that are shared/reused between Gemm2 and Gemm3

Application	Opt1 (baseline)	Opt2	Opt3	Opt4	Opt5
Autoencoder	2.98E+7 (1.00×)	7.44E+6 (4.00×)	1.19E+6 (24.91×)	5.06E+5 (58.80×)	3.92E+4 (759.47×)
Residual MLP	1.84E+7 (1.00×)	4.60E+6 (3.99×)	6.75E+5 (27.19×)	3.83E+5 (47.98×)	3.98E+4 (461.40×)
Residual Block	5.79E+7 (1.00×)	7.95E+6 (7.28×)	7.25E+6 (7.99×)	2.09E+6 (27.70×)	2.09E+6 (27.67×)
DWSConv. Block	6.63E+6 (1.00×)	1.04E+6 (6.37×)	3.32E+5 (19.98×)	1.35E+5 (49.26×)	1.35E+5 (49.26×)
Feed Forward	6.73E+7 (1.00×)	1.68E+7 (4.00×)	1.05E+6 (63.85×)	1.31E+5 (511.74×)	6.60E+4 (1019.39×)
Multi-Head Self Attention	1.05E+7 (1.00×)	2.69E+6 (3.91×)	2.68E+5 (39.34×)	3.95E+4 (266.82×)	3.51E+4 (299.67×)
3mm	6.38E+7 (1.00×)	8.82E+6 (7.24×)	1.28E+6 (50.00×)	4.91E+4 (1300.42×)	4.91E+4 (1300.42×)
atax	1.28E+6 (1.00×)	3.19E+5 (4.00×)	3.38E+4 (37.84×)	2.18E+3 (586.08×)	2.18E+3 (586.08×)
7mm Balanced	1.15E+6 (1.00×)	2.86E+5 (4.00×)	6.66E+4 (17.21×)	5.68E+3 (201.52×)	5.68E+3 (201.52×)
7mm Imbalanced	4.29E+6 (1.00×)	1.08E+6 (3.96×)	1.15E+5 (37.44×)	5.16E+4 (83.17×)	1.00E+4 (427.74×)
Geo. Mean	1.00×	4.70×	28.31×	152.30×	314.89×

Table 10: RTL Simulation Cycle Counts under Different Optimization Levels of Stream-HLS using 2560 DSPs Limit

separate MINLPs. This optimization yields even better performance, ranging between 27.7× and 1300.42×. Finally, **Opt5**, which combine both graph/node-level pipelining and node-level parallelization in a single MINLP results in the best performance, with speedups ranging between 27.67× and 1300.42× with a geometric mean of 314.89× compared to 152.30× for **Opt4** designs. As expected, in some cases solving the two MINLPs can lead to sub-optimal designs due to the conflict between the graph/node-level pipelining and node-level parallelization optimizations as shown in the MLP and transformer designs. Based on our observations, we noticed that solving the two MINLPs separately usually leads to the same solutions found by the combined approach when the workloads are balanced, i.e., the number of computations per node are similar. Thus, we created two synthetic applications one with balanced nodes (7mm Balanced), and the second one with imbalanced nodes (7mm Imbalanced), and the results seem to confirm this.

6 Related Work

A plethora of research has been conducted to automate and abstract the design of hardware circuits. Multiple studies have focused on design space exploration of pragma/directive insertion (mainly pipelining, array partitioning, and unrolling) for HLS such as [2, 20, 45, 47, 48, 63]. However, as shown in this work, the design space of hardware designs is much larger including for example code transformation and graph-level pipelining.

Other studies proposed stand-alone HLS compilers such as the open-source LegUp [7, 8] compiler and the Dynamic [26, 27] compiler for dynamically-scheduled circuits suitable for irregular and control-dominated workloads. Other efforts developed Python-based abstraction frameworks that are built on top of commercial HLS tools such as PyLog [24], HeteroCL [30], DaCe [4], and Allo [11]. Similarly, TAPA [13] developed an open-source C++ library on top of Vitis HLS [57] for streaming dataflow designs, while Dahlia [40] introduced a programming language with type-checking for predictable hardware execution of affine kernels. Other projects introduced intermediate representations and compilers suitable for hardware accelerators such as Spatial [29], Calyx [41], HIR [37], and multiple other efforts in the CIRCT project [1]. These efforts are orthogonal to Stream-HLS automation and design space exploration.

Another line of work is automatic accelerator generation. Multiple accelerator generation frameworks have been proposed for

single-kernel applications such as PolySA [17], AutoSA [53], and SuSy [31] for systolic arrays. POLSCA [64], ScaleHLS [58], HIDA [59], and POM [61] are more general MLIR-based frameworks for affine kernels, but they lack streaming capabilities.

Other streaming-related works include FBLAS [18], a streaming-based HLS library for linear algebra and Fleet [49] for composing and parallelizing a user’s RTL processing units using streams. Additionally, Darkroom [22], SODA [12], and Clockwork [25] proposed automatic compilers for stencil/image processing kernels, which we plan to inspire from to support stencils in Stream-HLS.

7 Future Work

The design space we discussed in this paper focuses on the scheduling and parallelization of multi-kernel applications. Stream-HLS as well as the prior works [11, 30, 58, 59, 61] we compared it with in Table 7 assume that input and output data come from fast partitioned on-chip memories, which may not be suitable for many use cases. We are currently working on expanding our formulation and DSE to consider the limited bandwidth of DDR and HBM channels, including data reuse and on-chip/off-chip communication tradeoffs. We are also working on extending Stream-HLS to support stencils and image processing applications similar to [12, 22, 25].

8 Conclusion

In this paper, we introduce a novel approach for transforming sequential multi-kernel applications into parallelized dataflow architectures. We propose an accurate performance model for dataflow architectures considering both shared buffer and FIFO for inter-task communication. This model is utilized to optimize application scheduling, enhancing node and graph-level pipelining and node-level parallelization. Our methodology is implemented as an automated framework called Stream-HLS, built on the MLIR infrastructure and incorporating various optimization passes. Stream-HLS designs yield considerable speedups compared to manually and automatically optimized designs of prior SOTA frameworks.

9 Acknowledgment and Disclosure

This work was partially supported by NSF awards CCF-1937599 and CCF-2211557, the CDSC industrial partners, the AMD³ HACC Programs, and the PRISM Center under the JUMP2.0 Program sponsored by Semiconductor Research Corporation (SRC) and DARPA.

³Jason Cong has a financial interest in AMD.

References

- [1] 2024. Circuit IR Compilers and Tools. <https://cirtc.llvm.org/>.
- [2] Yunsheng Bai, Atefeh Sohrabzadeh, Yizhou Sun, and Jason Cong. 2022. Improving GNN-based accelerator design automation with meta learning. In *Proceedings of the 59th ACM/IEEE Design Automation Conference*. 1347–1350.
- [3] Suhail Basalama, Atefeh Sohrabzadeh, Jie Wang, Licheng Guo, and Jason Cong. 2023. FlexCNN: An End-to-End Framework for Composing CNN Accelerators on FPGA. *ACM Transactions on Reconfigurable Technology and Systems* 16, 2 (2023), 1–32.
- [4] Tal Ben-Nun, Johannes de Fine Licht, Alexandros N Ziogas, Timo Schneider, and Torsten Hoefer. 2019. Stateful dataflow multigraphs: A data-centric model for performance portability on heterogeneous architectures. In *Proceedings of the International Conference for High Performance Computing, Networking, Storage and Analysis*. 1–14.
- [5] Mark Bohr. 2007. A 30 year retrospective on Dennard’s MOSFET scaling paper. *IEEE Solid-State Circuits Society Newsletter* 12, 1 (2007), 11–13.
- [6] Uday Bondhugula, Albert Hartono, Jagannathan Ramanujam, and Ponnuswamy Sadayappan. 2008. A practical automatic polyhedral parallelizer and locality optimizer. In *Proceedings of the 29th ACM SIGPLAN Conference on Programming Language Design and Implementation*. 101–113.
- [7] Andrew Canis, Jongsok Choi, Mark Aldham, Victor Zhang, Ahmed Kammoona, Jason H. Anderson, Stephen Brown, and Tomasz Czajkowski. 2011. LegUp: high-level synthesis for FPGA-based processor/accelerator systems (FPGA ’11). Association for Computing Machinery, New York, NY, USA, 33–36. <https://doi.org/10.1145/1950413.1950423>
- [8] Andrew Canis, Jongsok Choi, Blair Fort, Ruolong Lian, Qijing Huang, Nazanin Calagar, Marcel Gort, Jia Jun Qin, Mark Aldham, Tomasz Czajkowski, Stephen Brown, and Jason Anderson. 2013. From software to accelerators with LegUp high-level synthesis. In *2013 International Conference on Compilers, Architecture and Synthesis for Embedded Systems (CASES)*. 1–9. <https://doi.org/10.1109/CASES.2013.6662524>
- [9] David Castells-Rufas, Santiago Marco-Sola, Juan Carlos Moure, Quim Aguado, and Antonio Espinosa. 2022. FPGA acceleration of pre-alignment filters for short read mapping with HLS. *IEEE Access* 10 (2022), 22079–22100.
- [10] Adrian M. Caulfield, Eric S. Chung, Andrew Putnam, Hari Angepat, Jeremy Fowers, Michael Haselman, Stephen Heil, Matt Humphrey, Puneet Kaur, Joo-Young Kim, Daniel Lo, Todd Massengill, Kalin Ovtcharov, Michael Papamichael, Lisa Woods, Sitaram Lanka, Derek Chiou, and Doug Burger. 2016. A cloud-scale acceleration architecture. In *2016 49th Annual IEEE/ACM International Symposium on Microarchitecture (MICRO)*. 1–13. <https://doi.org/10.1109/MICRO.2016.7783710>
- [11] Hongzheng Chen, Niansong Zhang, Shaojie Xiang, Zhichen Zeng, Mengjia Dai, and Zhiru Zhang. 2024. Allo: A Programming Model for Composable Accelerator Design. *Proc. ACM Program. Lang.* 8, PLDI, Article 171 (jun 2024), 28 pages. <https://doi.org/10.1145/3656401>
- [12] Yuze Chi, Jason Cong, Peng Wei, and Peipei Zhou. 2018. SODA: Stencil with optimized dataflow architecture. In *2018 IEEE/ACM International Conference on Computer-Aided Design (ICCAD)*. IEEE, 1–8.
- [13] Yuze Chi, Licheng Guo, Jason Lau, Young-kyu Choi, Jie Wang, and Jason Cong. 2021. Extending high-level synthesis for task-parallel programs. In *2021 IEEE 29th Annual International Symposium on Field-Programmable Custom Computing Machines (FCCM)*. IEEE, 204–213.
- [14] Nitin Chugh, Vinay Vasista, Suresh Purini, and Uday Bondhugula. 2016. A DSL compiler for accelerating image processing pipelines on FPGAs. In *Proceedings of the 2016 International Conference on Parallel Architectures and Compilation*. 327–338.
- [15] Eric Chung, Jeremy Fowers, Kalin Ovtcharov, Michael Papamichael, Adrian Caulfield, Todd Massengill, Ming Liu, Daniel Lo, Shlomi Alkalay, Michael Haselman, Maleen Abeydeera, Logan Adams, Hari Angepat, Christian Boehn, Derek Chiou, Oren Firestein, Alessandro Forin, Kang Su Gatlin, Mahdi Ghandi, Stephen Heil, Kyle Holohan, Ahmad El Hussein, Tamas Juhasz, Kara Kagi, Ratna K. Kovvuri, Sitaram Lanka, Friedel van Megen, Dima Mukhortov, Prerak Patel, Brandon Perez, Amanda Rapsang, Steven Reinhardt, Bitu Rouhani, Adam Sapek, Raja Seera, Sangeetha Shekar, Balaji Sridharan, Gabriel Weisz, Lisa Woods, Phillip Yi Xiao, Dan Zhang, Ritchie Zhao, and Doug Burger. 2018. Serving DNNs in Real Time at Datacenter Scale with Project Brainwave. *IEEE Micro* 38, 2 (2018), 8–20. <https://doi.org/10.1109/MM.2018.022071131>
- [16] Jason Cong, Jason Lau, Gai Liu, Stephen Neuendorffer, Peichen Pan, Kees Vissers, and Zhiru Zhang. 2022. FPGA HLS today: successes, challenges, and opportunities. *ACM Transactions on Reconfigurable Technology and Systems (TRETS)* 15, 4 (2022), 1–42.
- [17] Jason Cong and Jie Wang. 2018. PolySA: Polyhedral-based systolic array auto-compilation. In *2018 IEEE/ACM International Conference on Computer-Aided Design (ICCAD)*. IEEE, 1–8.
- [18] Tiziano De Matteis, Johannes de Fine Licht, and Torsten Hoefer. 2020. FBLAS: Streaming linear algebra on FPGA. In *SC20: International conference for high performance computing, networking, storage and analysis*. IEEE, 1–13.
- [19] Robert H Dennard, Jin Cai, and Arvind Kumar. 2018. A perspective on today’s scaling challenges and possible future directions. In *Handbook of Thin Film Deposition*. Elsevier, 3–18.
- [20] Lorenzo Ferretti, Giovanni Ansaloni, and Laura Pozzi. 2018. Lattice-traversing design space exploration for high level synthesis. In *2018 IEEE 36th International Conference on Computer Design (ICCD)*. IEEE, 210–217.
- [21] Kaiming He, Xiangyu Zhang, Shaoqing Ren, and Jian Sun. 2016. Deep residual learning for image recognition. In *Proceedings of the IEEE Conference on Computer Vision and Pattern Recognition*. 770–778.
- [22] James Hegarty, John S Brunhaver, Zachary DeVito, Jonathan Ragan-Kelley, Noy Cohen, Steven Bell, Artem Vasilyev, Mark Horowitz, and Pat Hanrahan. 2014. Darkroom: compiling high-level image processing code into hardware pipelines. *ACM Trans. Graph.* 33, 4 (2014), 144–1.
- [23] Andrew G Howard, Menglong Zhu, Bo Chen, Dmitry Kalenichenko, Weijun Wang, Tobias Weyand, Marco Andreetto, and Hartwig Adam. 2017. Mobilenets: Efficient convolutional neural networks for mobile vision applications. *arXiv preprint arXiv:1704.04861* (2017).
- [24] Sitao Huang, Kun Wu, Hyunmin Jeong, Chengyue Wang, Deming Chen, and Wen-Mei Hwu. 2021. Pylog: An algorithm-centric python-based FPGA programming and synthesis flow. *IEEE Trans. Comput.* 70, 12 (2021), 2015–2028.
- [25] Dillon Huff, Steve Dai, and Pat Hanrahan. 2021. Clockwork: Resource-efficient static scheduling for multi-rate image processing applications on FPGAs. In *2021 IEEE 29th Annual International Symposium on Field-Programmable Custom Computing Machines (FCCM)*. IEEE, 186–194.
- [26] Lana Josipovic, Andrea Guerrieri, and Paolo Ienne. 2021. Synthesizing General-Purpose Code Into Dynamically Scheduled Circuits. *IEEE Circuits and Systems Magazine* 21, 2 (2021), 97–118. <https://doi.org/10.1109/MCAS.2021.3071631>
- [27] Lana Josipović, Andrea Guerrieri, and Paolo Ienne. 2022. From C/C++ Code to High-Performance Dataflow Circuits. *IEEE Transactions on Computer-Aided Design of Integrated Circuits and Systems* 41, 7 (2022), 2142–2155. <https://doi.org/10.1109/TCAD.2021.3105574>
- [28] Norman P. Jouppi, Cliff Young, Nishant Patil, David Patterson, Gaurav Agrawal, Raminder Bajwa, Sarah Bates, Suresh Bhatia, Nan Boden, Al Borchers, Rick Boyle, Pierre-luc Cantin, Clifford Chao, Chris Clark, Jeremy Coriell, Mike Daley, Matt Dau, Jeffrey Dean, Ben Gelb, Tara Vazir Ghaemmaghami, Rajendra Gottipati, William Gulland, Robert Hagmann, C. Richard Ho, Doug Hogberg, John Hu, Robert Hundt, Dan Hurt, Julian Ibarz, Aaron Jaffey, Alek Jaworski, Alexander Kaplan, Harshit Khaitan, Daniel Killebrew, Andy Koch, Naveen Kumar, Steve Lacy, James Laudon, James Law, Diemthu Le, Chris Leary, Zhuyuan Liu, Kyle Lucke, Alan Lundin, Gordon MacKean, Adriana Maggiore, Maire Mahony, Kieran Miller, Rahul Nagarajan, Ravi Narayanaswami, Ray Ni, Kathy Nix, Thomas Norrie, Mark Omernick, Narayana Penukonda, Andy Phelps, Jonathan Ross, Matt Ross, Amir Salek, Emad Samadiani, Chris Severn, Gregory Sizikov, Matthew Snelham, Jed Souter, Dan Steinberg, Andy Swing, Mercedes Tan, Gregory Thorson, Bo Tian, Horia Toma, Erick Tuttle, Vijay Vasudevan, Richard Walter, Walter Wang, Eric Wilcox, and Doe Hyun Yoon. 2017. In-Datacenter Performance Analysis of a Tensor Processing Unit. *SIGARCH Comput. Archit. News* 45, 2 (jun 2017), 1–12. <https://doi.org/10.1145/3140659.3080246>
- [29] David Koeplinger, Matthew Feldman, Raghu Prabhakar, Yaqi Zhang, Stefan Hadjis, Ruben Fiszal, Tian Zhao, Luigi Nardi, Ardavan Pedram, Christos Kozyrakis, and Kunle Olukotun. 2018. Spatial: a language and compiler for application accelerators. *SIGPLAN Not.* 53, 4 (jun 2018), 296–311. <https://doi.org/10.1145/3296979.3192379>
- [30] Yi-Hsiang Lai, Yuze Chi, Yuwei Hu, Jie Wang, Cody Hao Yu, Yuan Zhou, Jason Cong, and Zhiru Zhang. 2019. HeteroCL: A Multi-Paradigm Programming Infrastructure for Software-Defined Reconfigurable Computing. In *Proceedings of the 2019 ACM/SIGDA International Symposium on Field-Programmable Gate Arrays (Seaside, CA, USA) (FPGA ’19)*. Association for Computing Machinery, New York, NY, USA, 242–251. <https://doi.org/10.1145/3289602.3293910>
- [31] Yi-Hsiang Lai, Hongbo Rong, Size Zheng, Weihao Zhang, Xiuping Cui, Yunshan Jia, Jie Wang, Brendan Sullivan, Zhiru Zhang, Yun Liang, Youhui Zhang, Jason Cong, Nithin George, Jose Alvarez, Christopher Hughes, and Pradeep Dubey. 2020. SuSy: A Programming Model for Productive Construction of High-Performance Systolic Arrays on FPGAs. In *2020 IEEE/ACM International Conference on Computer Aided Design (ICCAD)*. 1–9.
- [32] Chris Lattner and Vikram Adve. 2004. LLVM: A compilation framework for lifelong program analysis & transformation. In *International symposium on code generation and optimization, 2004. CGO 2004*. IEEE, 75–86.
- [33] Chris Lattner, Mehdi Amini, Uday Bondhugula, Albert Cohen, Andy Davis, Jacques Pienaar, River Riddle, Tatiana Shpeisman, Nicolas Vasilache, and Oleksandr Zinenko. 2020. MLIR: A compiler infrastructure for the end of Moore’s law. *arXiv preprint arXiv:2002.11054* (2020).
- [34] Chris Lattner, Mehdi Amini, Uday Bondhugula, Albert Cohen, Andy Davis, Jacques Pienaar, River Riddle, Tatiana Shpeisman, Nicolas Vasilache, and Oleksandr Zinenko. 2021. MLIR: Scaling compiler infrastructure for domain specific computation. In *2021 IEEE/ACM International Symposium on Code Generation and Optimization (CGO)*. IEEE, 2–14.
- [35] llvm. 2023. Torch-MLIR Project. <https://github.com/llvm/torch-mlir>.

- [36] Michael Lo, Zhenman Fang, Jie Wang, Peipei Zhou, Mau-Chung Frank Chang, and Jason Cong. 2020. Algorithm-hardware co-design for BQSR acceleration in genome analysis toolkit. In *2020 IEEE 28th Annual International Symposium on Field-Programmable Custom Computing Machines (FCCM)*. IEEE, 157–166.
- [37] Kingshuk Majumder and Uday Bondhugula. 2023. HIR: An mlir-based intermediate representation for hardware accelerator description. In *Proceedings of the 28th ACM International Conference on Architectural Support for Programming Languages and Operating Systems, Volume 4*. 189–201.
- [38] William S Moses, Lorenzo Chelini, Ruizhe Zhao, and Oleksandr Zinenko. 2021. Polygeist: Raising C to polyhedral MLIR. In *2021 30th International Conference on Parallel Architectures and Compilation Techniques (PACT)*. IEEE, 45–59.
- [39] Fahad Bin Muslim, Liang Ma, Mehdi Roozmeh, and Luciano Lavagno. 2017. Efficient FPGA implementation of OpenCL high-performance computing applications via high-level synthesis. *IEEE Access* 5 (2017), 2747–2762.
- [40] Rachit Nigam, Sachille Atapattu, Samuel Thomas, Zhijing Li, Theodore Bauer, Yuwei Ye, Apurva Koti, Adrian Sampson, and Zhiru Zhang. 2020. Predictable accelerator design with time-sensitive affine types. In *Proceedings of the 41st ACM SIGPLAN Conference on Programming Language Design and Implementation*. 393–407.
- [41] Rachit Nigam, Samuel Thomas, Zhijing Li, and Adrian Sampson. 2021. A compiler infrastructure for accelerator generators. In *Proceedings of the 26th ACM International Conference on Architectural Support for Programming Languages and Operating Systems*. 804–817.
- [42] Ampl Optimization. 2024. <https://ampl.com/>.
- [43] Gurobi Optimization. 2024. <https://www.gurobi.com/downloads/ampl-and-gurobi/>.
- [44] Louis-Noël Pouchet and Tomofumi Yuki. 2012. Polybench: The polyhedral benchmark suite. URL: <http://www.cs.ucla.edu/pouchet/software/polybench> (2012).
- [45] Stéphane Pouget, Louis-Noël Pouchet, and Jason Cong. 2024. Automatic Hardware Pragma Insertion in High-Level Synthesis: A Non-Linear Programming Approach. *arXiv preprint arXiv:2405.12304* (2024).
- [46] Robert R Schaller. 1997. Moore’s law: past, present and future. *IEEE Spectrum* 34, 6 (1997), 52–59.
- [47] Atefeh Sohrabizadeh, Yunsheng Bai, Yizhou Sun, and Jason Cong. 2023. Robust GNN-based representation learning for HLS. In *2023 IEEE/ACM International Conference on Computer Aided Design (ICCAD)*. IEEE, 1–9.
- [48] Atefeh Sohrabizadeh, Cody Hao Yu, Min Gao, and Jason Cong. 2022. AutoDSE: Enabling software programmers to design efficient FPGA accelerators. *ACM Transactions on Design Automation of Electronic Systems (TODAES)* 27, 4 (2022), 1–27.
- [49] James Thomas, Pat Hanrahan, and Matei Zaharia. 2020. Fleet: A framework for massively parallel streaming on FPGAs. In *Proceedings of the Twenty-Fifth International Conference on Architectural Support for Programming Languages and Operating Systems*. 639–651.
- [50] Yaman Umuroglu, Nicholas J Fraser, Giulio Gambardella, Michaela Blott, Philip Leong, Magnus Jahre, and Kees Vissers. 2017. FINN: A framework for fast, scalable binarized neural network inference. In *Proceedings of the 2017 ACM/SIGDA International Symposium on Field-programmable Gate Arrays*. 65–74.
- [51] Ashish Vaswani, Noam Shazeer, Niki Parmar, Jakob Uszkoreit, Llion Jones, Aidan N Gomez, Lukasz Kaiser, and Illia Polosukhin. 2017. Attention is all you need. *Advances in Neural Information Processing Systems* 30 (2017).
- [52] Pascal Vincent, Hugo Larochelle, Isabelle Lajoie, Yoshua Bengio, Pierre-Antoine Manzagol, and Léon Bottou. 2010. Stacked denoising autoencoders: Learning useful representations in a deep network with a local denoising criterion. *Journal of machine learning research* 11, 12 (2010).
- [53] Jie Wang, Licheng Guo, and Jason Cong. 2021. AutoSA: A polyhedral compiler for high-performance systolic arrays on FPGA. In *The 2021 ACM/SIGDA International Symposium on Field-Programmable Gate Arrays*. 93–104.
- [54] Dennis Weller, Fabian Oboril, Dimitar Lukarski, Juergen Becker, and Mehdi Tahoori. 2017. Energy efficient scientific computing on FPGAs using OpenCL. In *Proceedings of the 2017 ACM/SIGDA International Symposium on Field-Programmable Gate Arrays*. 247–256.
- [55] AMD Xilinx. [n. d.]. Alveo U280 Data Center Accelerator Card. <https://www.xilinx.com/publications/product-briefs/alveo-u280-product-brief.pdf>.
- [56] AMD Xilinx. 2023. Merlin. <https://github.com/Xilinx/merlin-compiler>.
- [57] AMD Xilinx. 2023. Vitis High-Level Synthesis. <https://www.xilinx.com/products/design-tools/vitis.html>.
- [58] Hanchen Ye, Cong Hao, Jianyi Cheng, Hyunmin Jeong, Jack Huang, Stephen Neuendorffer, and Deming Chen. 2022. Scalehls: A new scalable high-level synthesis framework on multi-level intermediate representation. In *2022 IEEE International Symposium on High-Performance Computer Architecture (HPCA)*. IEEE, 741–755.
- [59] Hanchen Ye, Hyegang Jun, and Deming Chen. 2024. HIDA: A Hierarchical Dataflow Compiler for High-Level Synthesis. In *Proceedings of the 29th ACM International Conference on Architectural Support for Programming Languages and Operating Systems, Volume 1*. 215–230.
- [60] Chen Zhang, Guangyu Sun, Zhenman Fang, Peipei Zhou, and Jason Cong. 2023. Caffeine: Towards uniformed representation and acceleration for deep convolutional neural networks. In *Proceedings of the ACM Turing Award Celebration Conference-China 2023*. 47–48.
- [61] Weichuang Zhang, Jieru Zhao, Guan Shen, Quan Chen, Chen Chen, and Minyi Guo. 2024. An Optimizing Framework on MLIR for Efficient FPGA-based Accelerator Generation. In *2024 IEEE International Symposium on High-Performance Computer Architecture (HPCA)*.
- [62] Yichi Zhang, Junhao Pan, Xinheng Liu, Hongzheng Chen, Deming Chen, and Zhiru Zhang. 2021. FracBNN: Accurate and FPGA-efficient binary neural networks with fractional activations. In *The 2021 ACM/SIGDA International Symposium on Field-Programmable Gate Arrays*. 171–182.
- [63] Jieru Zhao, Liang Feng, Sharad Sinha, Wei Zhang, Yun Liang, and Bingsheng He. 2017. COMBA: A comprehensive model-based analysis framework for high level synthesis of real applications. In *2017 IEEE/ACM International Conference on Computer-Aided Design (ICCAD)*. IEEE, 430–437.
- [64] Ruizhe Zhao, Jianyi Cheng, Wayne Luk, and George A Constantinides. 2022. POLSCA: Polyhedral high-level synthesis with compiler transformations. In *2022 32nd International Conference on Field-Programmable Logic and Applications (FPL)*. IEEE, 235–242.